PHYSICAL REVIEW B **96**, 201302(R) (2017)

Volkov-Pankratov states in topological heterojunctions

S. Tchoumakov,[1] V. Jouffrey,[2] A. Inhofer,[3] E. Bocquillon,[3] B. Plaçais,[3] D. Carpentier,[2] and M. O. Goerbig[1]

[1]*Laboratoire de Physique des Solides, CNRS UMR 8502, Université Paris-Sud, Université Paris-Saclay, F-91405 Orsay Cedex, France*

[2]*Université de Lyon, ENS de Lyon, Université Claude Bernard, CNRS, Laboratoire de Physique, F-69342 Lyon, France*

[3]*Laboratoire Pierre Aigrain, Département de physique de l'ENS, Ecole normale supérieure, PSL Research University, Université Paris Diderot, Sorbonne Paris Cité, Sorbonne Universités, UPMC Université Paris 06, CNRS, 75005 Paris, France*

(Received 3 May 2017; published 1 November 2017)

We show that a smooth interface between two insulators of opposite topological $\mathbb{Z}_2$ indices possesses multiple surface states, both massless and massive. While the massless surface state is nondegenerate, chiral and insensitive to the interface potential, the massive surface states only appear for a sufficiently smooth heterojunction. The surface states are particle-hole symmetric and a voltage drop reveals their intrinsic relativistic nature, similarly to Landau bands of Dirac electrons in a magnetic field. We discuss the relevance of the massive Dirac surface states in recent angle-resolved photoemission spectroscopy and transport experiments.

DOI: 10.1103/PhysRevB.96.201302

Topological gapped phases are fascinating new states of matter. Their hallmark is the existence of gapless chiral states at their surface that have been probed in topological insulators by angle-resolved photoemission spectroscopy (ARPES) [1–3], transport [4,5] and scanning tunneling microscopy (STM) [6] measurements. Our common understanding of their existence lies in the necessary gap closing at the interface between two insulators characterized by different topological invariants [7–9]. Moreover, the same experiments that detect these gapless states also evidence multiple massive surface states in both the conduction and valence bands. These additional surface states have been attributed to conventional properties of the interface, such as band bending, unrelated to the topological nature of the insulators. Indeed, previous studies consider that the amplitude of band bending is strong enough to confine states in both the conduction and the valence bands [1,2,10]. From this point of view, one would consider the two types of surface states to be of different origin: topological for the massless states and due to strong band bending for the massive ones.

Here we show that this is not necessarily the case. We describe the interface between a topological and a normal insulator or vacuum, which is a *topological heterojunction* (THJ), within a model where the gap inversion occurs over a finite interface size ℓ, and we show that it hosts multiple surface states, both massless and massive. In the limit of a wide interface, where ℓ is much larger than an intrinsic material-dependent length scale ξ, these states are similar to Landau bands of a Dirac material in a magnetic field. The gapless surface state is then analogous to the $n = 0$ Landau band and it only depends on the properties far away from the interface as in the Aharonov-Casher argument [11,12]. Furthermore, as for Landau bands, the massive surface states appear in both the conduction and the valence bands and are sensitive to the details of the interface. Prior to the recent discussion within the context of topological insulators [9], massless and massive surface states at an interface with gap inversion were studied theoretically back in the 1980s by Volkov and Pankratov in a set of pioneering papers [13–15], albeit in the simplified framework of a symmetric interface. We thus call such massive surface states *Volkov-Pankratov states* (VPS). In this Rapid Communication, we stress the topological origin of this type of confinement which is tightly related to relativistic physics and inherently different from confinement in a conventional quantum well. Moreover, we characterize the properties of the surface states as a function of various properties of the THJ, such as a gap asymmetry between the two materials and surface band bending.

We consider the interface between two semiconductors with inverted, $\Delta_1 < 0$, and conventional, $\Delta_2 > 0$, gaps in the simplest situation where both gaps are located at a single point of the Brillouin zone, e.g., the Γ point. Hence we model each insulating phase with the generic $k \cdot P$ Hamiltonian around the Γ point, describing in particular Bi_2Se_3 [9],

$$\hat{H}_0 = \mu \hat{\mathbb{1}} \otimes \hat{\mathbb{1}} + \Delta \hat{\mathbb{1}} \otimes \hat{\tau}_z + v_F k_z \hat{\mathbb{1}} \otimes \hat{\tau}_y + v_F (k_y \hat{\sigma}_x - k_x \hat{\sigma}_y) \otimes \hat{\tau}_x, \tag{1}$$

where we assume $v_F > 0$ and set $\hbar = 1$ hereafter. The $\hat{\sigma}$ and $\hat{\tau}$ Pauli matrices act, respectively, on spin and orbital subspaces. In a first place, μ is set to zero in both semiconductors. The spectrum of (1) consists of two doubly degenerate bands $\varepsilon_{\mathbf{k}}^{(\pm)} = \pm\sqrt{\Delta^2 + v_F^2 k^2}$ and the two insulators only differ by their band gaps Δ_1 and Δ_2.

We model the interface between the two insulators, chosen as normal to the z direction, by a z-dependent $k \cdot P$ Hamiltonian $\hat{H}_s$, which smoothly interpolates between the two bulk Hamiltonians over a characteristic size ℓ. This amounts to replacing Δ in Eq. (1) with a smoothly interpolating gap $\Delta(z)$, such that $\Delta(z \to -\infty) = \Delta_1$ and $\Delta(z \to +\infty) = \Delta_2$. In addition to the interface width ℓ, one finds a natural length $\xi = 2v_F/|\Delta_1 - \Delta_2|$, and for a smooth interface one has $\ell > \xi$, while for a sharp interface $\ell < \xi$. The interface width ℓ depends on the material and growth technique but we expect that a smooth interface generically occurs between a small gap topological insulator such as Bi_2Se_3 ($2\Delta_1 = -0.35$ eV [1], $v_F = 2.5$ eV Å [16]) and a large gap insulator such as HfO_2 ($2\Delta_2 = 5$ eV) since then $\xi \sim 2$ Å is rather small. On the other hand, for the interface between two small gap insulators, with, e.g., $2\Delta \sim 0.25$ eV, we estimate $\xi \sim 2$ nm and thus, depending on ℓ, there can be either a smooth or a sharp interface [17].

A convenient choice to describe the z-dependent gap around the THJ is $\Delta(z) = \frac{1}{2}(\Delta_2 - \Delta_1)[\delta + \tanh(z/\ell)]$, where we have introduced the *gap asymmetry* $\delta = (\Delta_1 + \Delta_2)/(\Delta_2 - \Delta_1)$. The situation with opposite gaps, $\delta = 0$, for which the

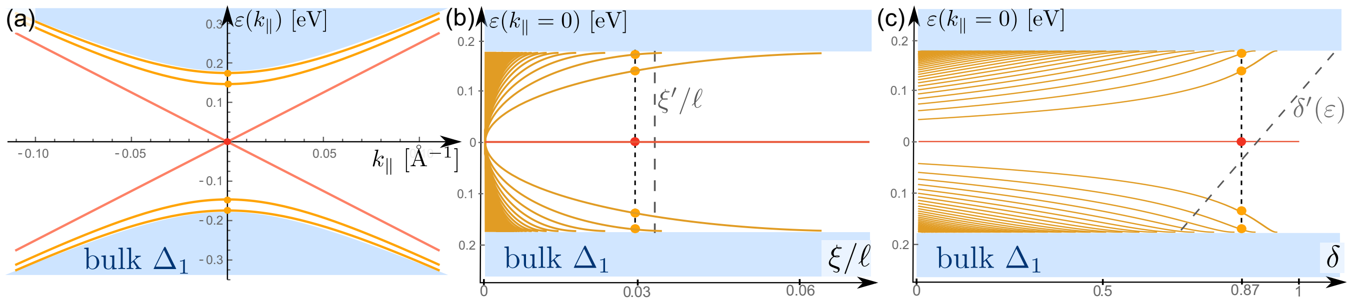

FIG. 1. (a) Surface states obtained for $2\Delta_1 = -0.35$ eV, $2\Delta_2 = 5$ eV, $v_F = 2.5$ eV Å, and $\ell = 6$ nm. The corresponding reduced parameters are $\delta = 0.87$ and $\xi/\ell = 0.03$. We show the band dispersion of the gapless surface state (red), the massive surface states (orange), and the bulk states (blue). (b),(c) Gaps of the surface states (orange) for $v_F = 2.5$ eV Å, $2\Delta_1 = -0.35$ eV, and (b) as a function of the sharpness of the interface ξ/ℓ with $\delta = 0.87$ and (c) as a function of the gap asymmetry δ with $\xi/\ell = 0.03$. An applied electric field renormalizes the values of ξ and δ (gray dashed lines), as a function of energy for δ.

Schrödinger equation resembles the Pöschl-Teller equation [18], was studied in Refs. [13–15]. Here, we solve the more relevant situation with $\delta \neq 0$ with the use of hypergeometric functions (see Supplemental Material [19]). This yields the spectrum of surface states,

$$\varepsilon_{n,\pm}(k_x,k_y) = \pm v_F\sqrt{k_x^2 + k_y^2 + 1/\ell_n^2}, \tag{2}$$

where the characteristic length ℓ_n of each mode in the z direction is

$$\frac{1}{\ell_n^2} = \frac{2n}{\ell\xi}\left(1 - n\frac{\xi}{2\ell}\right)\left[1 - \left(\frac{\delta}{1 - n\frac{\xi}{\ell}}\right)^2\right], \tag{3}$$

which depends on the integer values n delimited by

$$n < N = \frac{\ell}{\xi}(1 - \sqrt{|\delta|}). \tag{4}$$

The corresponding band dispersions are illustrated in Fig. 1(a) with the $n = 0$ state in red and the $n \geqslant 1$ states in orange. The inequality (4) yields surface states only if $|\delta| < 1$, i.e., if the two semiconductors have gaps of opposite sign. Moreover, as illustrated in Fig. 1(b), the number of states depends on the THJ geometry with many massive ($N \geqslant 1$) hole- *and* electronlike surface states for a smooth interface, but with only the single massless $n = 0$ surface state for a sharp interface. This kind of quantization is reminiscent of that in a uniform magnetic field which happens to be analog to the limit of a linearized potential for $\ell \gg \xi$, which we discuss in the Supplemental Material [19] and which was already discussed in the context of Majorana surface states in Refs. [20–22]. Note that the occurrence of the additional VPS still fulfills the topological $\mathbb{Z}_2$ constraint [23] since the $n = 0$ state is simply degenerate, while the VPS ($n \geqslant 1$) are doubly degenerate, such that the parity of the number of surface states is unchanged. We stress that the existence of both the massless and the massive surface states requires the heterojunction to be topological, $\Delta_1\Delta_2 < 0$, in contrast to standard band-bending massive surface states.

The peculiar nature of the VPS is further illustrated by their response to an electric field applied perpendicular to the interface. We expect the number of VPS, expressed in Eq. (4), to be small since their band gap has to be smaller than the smallest bulk band gap, $\min(|\Delta_1|,|\Delta_2|)$, and that a large gap asymmetry δ decreases their number as illustrated in Fig. 1(c).

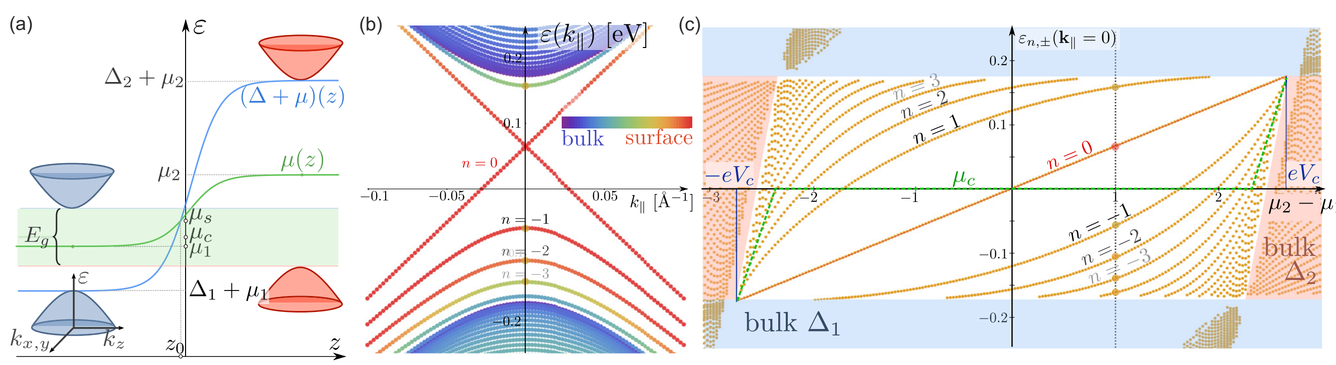

FIG. 2. Surface states of a THJ with n- and p-doped insulators. (a) Sketch of the heterojunction with a $\mu_2 - \mu_1$ drop in the chemical potential. The pn junction is characterized by a chemical potential μ_c and a band gap common to both insulators (shaded green region) of size $E_g = |\Delta_2 - \Delta_1 - (\mu_2 - \mu_1)|$, which vanishes for a large chemical potential or voltage drop, defining a breakdown voltage. The surface states are centered around the position z_0 where the gap vanishes, with surface chemical potential $\mu_S \approx \mu(z_0) = \frac{1}{2}(\mu_1 + \mu_2) - \frac{1}{2}(\mu_2 - \mu_1)\delta$. (b) Spectrum obtained by numerical simulation with the same parameters as in Fig. 1, $f(z/\ell) = \tanh(z/\ell)$, and centered around the band gap of the inverted insulator (blue). We use $\mu_2 - \mu_1 = 1$ eV, and the colors represent the amplitude of surface density $\rho_S \approx |\Psi(z = z_0)|^2$ for each state. (c) Energy $\varepsilon_{n,\pm}(\mathbf{k}_\parallel = 0)$ of the surface states as a function of the chemical-potential difference $\mu_2 - \mu_1$. Multiple VPS appear in the valence band for $|\mu_2 - \mu_1|$ closer to $|eV_c| = |\Delta_2 - \Delta_1| = 2.675$ eV for a positive and strong gap asymmetry, $\delta = 0.87 \sim 1 = |\delta|_{\max}$.

However, we show below that the visibility of VPS can be strongly enhanced by an electric field, possibly originating from surface band bending due to chemical doping or an applied gate voltage under Dirac screening [24]. We consider a chemical potential μ in Eq. (1) that varies over the interface with the same profile $\mu(z) = \frac{1}{2}(\mu_2 - \mu_1)f(z/\ell)$ as the gap $\Delta(z)$, as depicted in Fig. 2(a), and with opposite potentials in each semiconductor. We account for this potential with a Lorentz boost (see Supplemental Material [25]) which shows that the surface states only exist if the relativistic parameter $\beta = -(\mu_2 - \mu_1)/(\Delta_2 - \Delta_1) \in [-1,1]$. This reminds one of the behavior of Landau levels in crossed electric and magnetic fields [26] with a typical electric field $\mathcal{E} = (\mu_2 - \mu_1)/e\ell$ that has to be smaller than a *critical electric field* $\mathcal{E}_c = (\Delta_2 - \Delta_1)/e\ell$, corresponding to a breakdown voltage $V_c = (\Delta_2 - \Delta_1)/e$, above which the surface states disappear. This critical behavior happens because the surface states exist within the band gap common to both semiconductors depicted in Fig. 2(a) and it vanishes above the breakdown voltage. For voltage drops below V_c, the Lorentz boost renormalizes the parameters in the Schrödinger equation $\hat{H}_s'|\Psi'\rangle = \varepsilon|\Psi'\rangle$ (see Supplemental Material [25]). The interface is sharpened by an increase in the intrinsic length as $\xi'/\xi = 1/\sqrt{1-\beta^2}$, while the effective gap asymmetry becomes

$$\delta' = \frac{1}{1-\beta^2}\left[\delta + \frac{\varepsilon(\mu_2 - \mu_1)/2}{(v_F/\xi)^2}\right], \tag{5}$$

and the effective Fermi velocity decreases as $v_F'/v_F = \sqrt{1-\beta^2}$. These renormalized parameters decrease the VPS band gaps (see Supplemental Material [25]) and alter their spectrum in a way that depends on the sign of the voltage drop $\mu_2 - \mu_1$, relative to the gap asymmetry δ. As shown in Fig. 1(c), the renormalized δ' is such that if $\mu_2 - \mu_1$ and $\Delta_2 - \Delta_1$ have the same signs, then increasing the voltage drop shifts up the spectrum of VPS and increases the number of particlelike VPS. This is the situation depicted in Fig. 2(c). Conversely, if $\mu_2 - \mu_1$ and $\Delta_2 - \Delta_1$ have opposite signs, an increasing electric field shifts down the VPS spectrum and increases the number of holelike VPS. This unique behavior is a hallmark of VPS in a THJ, revealing their intrinsic relativistic origin. The spectrum of surface states has to be obtained self-consistently if the original spectrum depends explicitly on δ, as in Eq. (2). This can be avoided in simplified models (see [4] and Supplemental Material [25]). Alternatively, we can directly solve a discretized version of Eq. (1) for a generic $\tanh(z/\ell)$ interface. The results are shown in Figs. 2(b) and 2(c) and confirm the unique effect of a voltage drop on the VPS of a THJ.

Let us comment on the intrinsic difference in nature between VPS in a THJ and conventional nonrelativistic states localized in a potential well at an interface. In both cases, the interface is described by a change in the gap $\Delta(z)$ for which the parity symmetry $\mathcal{P} = \hat{\sigma}_z \otimes \hat{\tau}_z$ leads to a particle-hole symmetric spectrum which is absent in the case of electrostatic confinement. Moreover, a general surface state $\Psi = (\phi_{1,+},\phi_{2,+},\phi_{1,-},\phi_{2,-})$ written over the eigenbasis of the parity operator $\mathcal{P}$, as in the Supplemental Material [19], can be determined by squaring the time-independent Schrödinger equation associated with Eq. (1). In doing so, we obtain

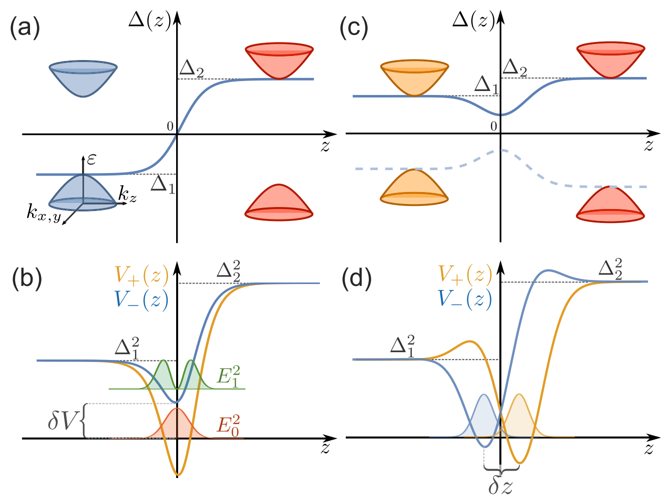

FIG. 3. Sketch of the position-dependent gap $\Delta(z)$ and the corresponding confining potentials $V_\pm(z)$ of the wave-function components $\Psi_\pm$. (a),(b) The case of band inversion (THJ) and (c),(d) the case of a gap minima $|\Delta(z)|$ in a conventional heterojunction. (b) The potentials minima are shifted in energy by $\delta V \sim v_F^2/\ell\xi$; (d) the potential minima are shifted in position by $\delta z \sim v_F/2\Delta_{\min}$. It is only in the case of a THJ that one finds a nondegenerate bound state for the V_- potential.

for each component $\phi_{i,s}$ ($i = 1,2$, $s = \pm$) a one-dimensional nonrelativistic Schrödinger equation,

$$\left[-v_F^2\partial_z^2 + V_s(z)\right]\phi_{i,s} = \left(\varepsilon^2 - v_F^2 k_\parallel^2\right)\phi_{i,s}, \tag{6}$$

with a potential $V_\pm(z) = \Delta(z)^2 \mp v_F\partial_z\Delta(z)$, and associated eigenvalues $E_n^2 = (\varepsilon^2 - v_F^2 k_\parallel^2)$. The chiral symmetry relates the two solutions associated with both $V_\pm(z)$ potentials via the relation $\phi_{i,s} = -[v_F\partial_z - s\Delta(z)]\phi_{i,-s}$. Thus every state is doubly degenerate except for the $n = 0$ surface state, which is analyzed in detail below and which we call the *chiral surface states* (CSS). These CSS are the topologically protected ones, which one obtains based on topological invariants and that survive in the limit where the interface becomes sharp, $\ell/\xi \to 0$. This means that the CSS are completely independent of the $\Delta(z)$ profile as shown by the Aharonov-Casher argument in the Supplemental Material [27]. In Fig. 3, we represent two situations for this Schrödinger equation: a THJ in Figs. 3(a) and 3(b) where $\Delta(z=0) = 0$ and a conventional heterojunction in Figs. 3(c) and 3(d) where there is no band inversion but a local minimum of the band gap $|\Delta(z)|$.

The physical properties of these surface states can be captured by an analysis of Eq. (6). In the THJ case, $V_+(z)$ necessarily has a minimum regardless of the interface size because $\Delta(z=0) = 0$ and thus $V_+(z=0) = -v_F\partial_z\Delta(z=0) < 0$. The associated bound state is then the CSS with $E_0 = 0$ whose nondegenerate nature manifests itself here by the fact that $V_-(z=0) = +v_F\partial_z\Delta(z=0) > 0$, precluding another $E = 0$ state. The existence of VPS necessitates that both $V_-(z)$ and $V_+(z)$ have a minimum because of the chiral symmetry, in particular this necessitates $V_-(0) < \min\{\Delta_1^2,\Delta_2^2\}$. One can estimate $V(z \sim 0) \sim v_F\partial_z\Delta(z=0) \sim v_F^2/\ell\xi$, such that the condition for appearance of VPS reads $v_F^2/\ell\xi < \min\{\Delta_1^2,\Delta_2^2\} = v_F^2(1-|\delta|)^2/\xi^2$, which agrees with Eq. (4) obtained for a particular choice of $\Delta(z)$ discussed above. This discussion can also be extended to a conventional heterojunction with no gap inversion, as studied in Refs. [5,28]. We expect bound states if the gap function $|\Delta(z)|$ has a minimum $|\Delta_{\min}| < \min\{|\Delta_1|,|\Delta_2|\}$, as depicted in Fig. 3(c). Indeed, Eq. (6) provides a pair of VPS shown in Fig. 3(d) since both potentials satisfy $V_{\pm,\min} \simeq \Delta_{\min}^2 < \min\{\Delta_1^2,\Delta_2^2\}$. In this case, all massive surface states are degenerate with a linear combinations of $|\pm\rangle$ states located on either side of the interface with a separation $\delta z \simeq v_F/2\Delta_{\min}$, similarly to the case of a thin confined insulator recently discussed in Ref. [5].

The above description of a THJ shows the existence of massive states intimately related to the relativistic and topological nature of the interface. While a clear determination of the nature of these surface states requires one to study their dependence on an external electric field, along the lines of Ref. [4] for strained bulk HgTe, their occurrence in previous ARPES experiments in Bi_2Se_3 and Bi_2Te_3 aged in an oxidizing atmosphere [2,3] can be critically discussed within our theory. While electrostatic band bending can reproduce the electronlike surface states, the holelike ones necessitate an associated energy scale larger than the bulk valence-band width, unlikely in particular in Bi_2Te_3 [3]. On the other hand, in our theoretical description, both electron- and holelike VPS arise on equal footing due to the underlying particle-hole symmetry in a THJ. In the experiments reported in Refs. [2,3], one observes two or three electron- and holelike surface states. For Bi_2Se_3, published values for $v_F = 2.3\ldots5$ eV Å [16,29] and $2\Delta = 350$ meV [1] yield a characteristic interface width $\xi \approx v_F/\Delta = 6.5\ldots23$ Å. In an oxidizing atmosphere, the depth of the oxide layer can be estimated as $\ell \approx 10\ldots20$ Å [30], which leads to an expected number of $N \approx \ell/\xi = 1\ldots3$ VPS, in agreement with experiments [2,3]. Moreover, we find $\ell_S = \sqrt{\ell\xi} \approx 8\ldots20$ Å and thus VPS energy gaps $\Delta_{\rm VPS} \approx v_F/\ell_S = 100\ldots600$ meV in reasonable agreement with [2,3]. In our theory, we expect similar band gaps for the electron- and holelike VPS which is observed experimentally in Bi_2Se_3, as we discuss in the Supplemental Material [31]. This is a strong indication of the topological origin of the surface states. The ARPES measurement of both the band gap and the Fermi velocity of VPS as a function of band bending could help one to get better insight into their relativistic nature. Moreover, we expect the absence of VPS for In-doped Bi_2Se_3 in an oxidizing atmosphere for a doping that turns the material into a normal semiconductor and which has been recently discussed in Ref. [32].

In conclusion, we have shown that THJs, characterized by a continuous gap inversion between two semiconductors, generically host massive surface states in addition to the usual massless chiral state. A condition for the existence of these VPS is a sufficiently smooth interface $\ell > \xi$ as compared to the material-dependent characteristic length $\xi = 2v_F/|\Delta_1 - \Delta_2|$ and a small gap asymmetry $\delta = (\Delta_1 + \Delta_2)/(\Delta_2 - \Delta_1)$. Both the massless and the massive surface states are intrinsically relativistic, revealed in the particle-hole symmetry of their spectrum as well as by the effect of electrostatic band bending. The surface states only persist below the breakdown voltage but the number of electron- or holelike surface states can be increased by band bending depending on the sign of the voltage drop with respect to the direction of increase in the gap. These surface states are reminiscent of Landau bands, in particular for a wide THJ ($\ell \gg \xi$). The existence of such VPS and their relativistic nature is relevant for recent ARPES measurements on aged Bi_2Se_3 and Bi_2Te_3 [1–3] and have been identified in transport measurements on strained bulk HgTe [4]. Uncovering the signature of these states and their electric-field dependence for other probes such as in tunneling spectroscopy is a natural and exciting perspective.

We would like to thank M. Civelli, B. A. Assaf, and C. Quay for fruitful discussions.

[1] M. Bianchi, D. Guan, S. Bao, J. Mi, B. B. Iversen, P. D. C. King, and P. Hofmann, Nat. Commun. **1**, 128 (2010).
[2] M. Bianchi, R. C. Hatch, J. Mi, B. B. Iversen, and P. Hofmann, Phys. Rev. Lett. **107**, 086802 (2011).
[3] C. Chen, S. He, H. Weng, W. Zhang, L. Zhao, H. Liu, X. Jia, D. Mou, S. Liu, J. He, Y. Peng, Y. Feng, Z. Xie, G. Liu, X. Dong, J. Zhang, X. Wang, Q. Peng, Z. Wang, S. Zhang, F. Yang, C. Chen, Z. Xu, X. Dai, Z. Fang, and X. J. Zhou, Proc. Natl. Acad. Sci. USA **109**, 3694 (2012).
[4] A. Inhofer, S. Tchoumakov, B. A. Assaf, G. Fève, J. M. Berroir, V. Jouffrey, D. Carpentier, M. O. Goerbig, B. Plaçais, K. Bendias, D. M. Mahler, E. Bocquillon, R. Schlereth, C. Brüne, H. Buhmann, and L. W. Molenkamp, Phys. Rev. B **96**, 195104 (2017).
[5] A. Barnerjee, A. Rai, K. Majhi, S. R. Barman, R. Ganesan, and P. S. A. Kumar, J. Phys.: Condens. Matter **29**, 185001 (2017).
[6] C. Mann, D. West, I. Miotkowski, Y. P. Chen, S. Zhang, and C.-K. Shih, Nat. Commun. **4**, 2277 (2013).
[7] X.-L. Qi and S.-C. Zhang, Rev. Mod. Phys. **83**, 1057 (2011).
[8] V. A. Volkov and V. V. Enaldiev, J. Exp. Theor. Phys. **122**, 608 (2016).
[9] F. Zhang, C. L. Kane, and E. J. Mele, Phys. Rev. B **86**, 081303(R) (2012).
[10] M. S. Bahramy, P. D. C. King, A. de la Torre, J. Chang, M. Shi, L. Patthey, G. Balakrishnan, P. Hofmann, R. Arita, N. Nagaosa, and F. Baumberger, Nat. Commun. **3**, 1159 (2012).
[11] Y. Aharonov and A. Casher, Phys. Rev. A **19**, 2461 (1979).
[12] T. Kawarabayashi, Y. Hatsugai, T. Morimoto, and H. Aoki, Phys. Rev. B **83**, 153414 (2011).
[13] V. Volkov and O. Pankratov, *Landau Level Spectroscopy*, edited by G. Landwehr and E. I. Rashba (North-Holland, Amsterdam, 1991), Chap. 14, pp. 819–852.
[14] B. A. Volkov and O. A. Pankratov, JETP Lett. **42**, 178 (1985).
[15] O. Pankratov, S. Pakhomov, and V. Volkov, Solid State Commun. **61**, 93 (1987).
[16] Y. Xia, D. Qian, D. Hsieh, L. Wray, A. Pal, H. Lin, A. Bansil, D. Grauer, Y. S. Hor, R. J. Cava, and M. Z. Hasan, Nat. Phys. **5**, 398 (2009).
[17] The width of the interface can, in principle, be derived within a mean-field approximation by choosing ℓ that minimizes the energy as in Ref. [33].

[18] J. Lekner, Am. J. Phys. **75**, 1151 (2007).
[19] See Supplemental Material at http://link.aps.org/supplemental/10.1103/PhysRevB.96.201302 for the surface states solutions, which includes Refs. [34–38].
[20] Y. Oreg, G. Refael, and F. von Oppen, Phys. Rev. Lett. **105**, 177002 (2010).
[21] A. M. Cook, M. M. Vazifeh, and M. Franz, Phys. Rev. B **86**, 155431 (2012).
[22] T. Karzig, G. Refael, and F. von Oppen, Phys. Rev. X **3**, 041017 (2013).
[23] M. Z. Hasan and C. L. Kane, Rev. Mod. Phys. **82**, 3045 (2010).
[24] C. Brüne, C. Thienel, M. Stuiber, J. Böttcher, H. Buhmann, E. G. Novik, C.-X. Liu, E. M. Hankiewicz, and L. W. Molenkamp, Phys. Rev. X **4**, 041045 (2014).
[25] See Supplemental Material at http://link.aps.org/supplemental/10.1103/PhysRevB.96.201302 for information on the Lorentz boost, which includes Refs. [39–44].
[26] V. Lukose, R. Shankar, and G. Baskaran, Phys. Rev. Lett. **98**, 116802 (2007).
[27] See Supplemental Material at http://link.aps.org/supplemental/10.1103/PhysRevB.96.201302 for the adaption of the Aharonov-Casher argument to the $n = 0$ chiral surface state, which includes Refs. [11,12].
[28] M. Kotulla and U. Zülicke, New J. Phys. **19**, 073025 (2017).
[29] L. He, F. Xiu, X. Yu, M. Teague, W. Jiang, Y. Fan, X. Kou, M. Lang, Y. Wang, G. Huang, N.-C. Yeh, and K. L. Wang, Nano Lett. **12**, 1486 (2012).
[30] A. J. Green, S. Dey, Y. Q. An, B. O'Brien, S. O'Mullane, B. Thiel, and A. C. Diebold, J. Vac. Sci. Technol. A **34**, 061403 (2016).
[31] See Supplemental Material at http://link.aps.org/supplemental/10.1103/PhysRevB.96.201302 for orders of magnitude .
[32] I. Belopolski, S.-Y. Xu, N. Koirala, C. Liu, G. Bian, V. N. Strocov, G. Chang, M. Neupane, N. Alidoust, D. Sanchez, H. Zheng, M. Brahlek, V. Rogalev, T. Kim, N. C. Plumb, C. Chen, F. Bertran, P. Le Fèvre, A. Taleb-Ibrahimi, M.-C. Asensio, M. Shi, H. Lin, M. Hoesch, S. Oh, and M. Z. Hasan, Sci. Adv. **3**, 1501692 (2017).
[33] W. P. Su, J. R. Schrieffer, and A. J. Heeger, Phys. Rev. B **22**, 2099 (1980).
[34] T. Prokopec, M. G. Schmidt, and J. Weenink, Phys. Rev. D **87**, 083508 (2013).
[35] F. R. Klinkhamer and L. Yang, Phys. Rev. D **91**, 045028 (2015).
[36] Y. Araki, A. Yoshida, and K. Nomura, Phys. Rev. B **94**, 115312 (2016).
[37] E. T. Whittaker and G. N. Watson, *A Course of Modern Analysis*, 4th ed. (Cambridge University Press, Cambridge, 1950), pp. 281–296.
[38] M. O. Goerbig, arXiv:0909.1998.
[39] S. Tchoumakov, M. Civelli, and M. O. Goerbig, Phys. Rev. B **95**, 125306 (2017).
[40] A. Díaz-Fernández, L. Chico, J. W. González, and F. Domínguez-Adame, Sci. Rep. **7**, 8058 (2017).
[41] N. Klier, S. Sharma, O. Pankratov, and S. Shallcross, arXiv:1702.08784.
[42] Z.-M. Yu, Y. Yao, and S. A. Yang, Phys. Rev. Lett. **117**, 077202 (2016).
[43] M. Udagawa and E. J. Bergholtz, Phys. Rev. Lett. **117**, 086401 (2016).
[44] S. Tchoumakov, M. Civelli, and M. O. Goerbig, Phys. Rev. Lett. **117**, 086402 (2016).